

Characterization of Nano-Scale Fine Precipitates in Al-Mg-Si Alloys for Automotive Applications

Makoto SAGA*¹Naoki MARUYAMA*¹

Abstract

Bake-hardenable Al-Mg-Si alloys are well used for the automotive body sheets. There are many reports concerned about the precipitation sequence in Al-Mg-Si alloys, although the chemical composition and the structure of the precipitates are not fully clarified. The purpose of this study is to investigate the chemical composition and the structure of the precipitates by using field emission transmission electron microscope equipped with energy dispersive X-ray spectroscopy (EDS).

1. Introduction

Aluminum alloys have come to be applied to automobile body panels to reduce car weight over the last years. While Al-Mg alloys have conventionally accounted for a good part of the car body application of aluminum alloys in Japan because of good formability, the latest trend is that Al-Mg-Si alloys, with which the body weight can be decreased further through the reduction of sheet thickness, are becoming the mainstream of the car body application of aluminum alloys thanks to good bake-hardenability. Nippon Steel Corporation has been developing aluminum alloys for automobile applications to offer the most suitable material in consideration of the above trend among carmakers.

The bake-hardenability of Al-Mg-Si alloys shows itself through precipitation hardening. Many studies are under way in Japan and abroad on the chemical composition and heat treatment methods of the alloys, aiming at increasing the amount of precipitation hardening under the restrictions of the heat treatment conditions of the paint baking processes in the present automobile production lines¹⁻⁴. It has been known that an excessive addition of Si to a balanced alloy of a pseudo-binary Al-Mg₂Si system significantly improves aging properties^{5,6}, and for this reason, most of the materials presently used for the application are of this type of excess-Si alloy.

It is very important for the design of a high-bake-hardenable alloy to collect information on the structure and chemical composition of the phases that precipitate during the paint baking process. There have been many studies also on the process of precipitation during aging. However, in spite of many reports that have been presented⁷⁻¹⁰,

the structure and chemical composition of the phases that precipitate during aging have not been made clear. This is presumably because the precipitates forming during the paint baking process are as fine as several nanometers in size at the largest and it is very difficult to examine them.

In view of the situation, the authors characterized the fine precipitates that are only nanometers in size as having an influence on the bake-hardenability of Al-Mg-Si alloys, using a field emission type transmission electron microscope (TEM) capable of obtaining information on the structure and chemical composition in a nanometer-scale region. The present paper reports the results.

2. Experimental Procedure

A balanced alloy (hereinafter referred to as Alloy A) having the chemical composition shown in **Table 1** with a Mg₂Si content of approximately 1% and an excess-Si alloy (hereinafter referred to as Alloy B) having a Si content in excess of that of Alloy A by approximately 0.5% were melted, subjected to a homogenizing treatment in the atmosphere at 803K for 46.8ks, and then hot and cold rolled into specimen sheets 1 mm in thickness.

The precipitation processes of an alloy having such a chemical composition are known to start from a supersaturated solid solution and follow the sequence of a G.P.I zone, an intermediate β'' phase, an intermediate β' phase and an equilibrium β phase. It is the intermediate β'' phase (a metastable phase) that contributes to the strengthening of the material through precipitation at 443 to 453K, the temperature range of the paint baking⁴. In view of the fact, for the purpose of characterizing mainly the β'' phase in comparison with the β'

*¹ Steel Research Laboratories

Table 1 Chemical compositions of specimen alloys (mass%)

	Mg	Fe	Si	Cr	Zn	Ti	Al	Mg ₂ Si	Excess Si
Balanced Alloy A	0.63	0.05	0.35	< 0.01	< 0.01	0.01	Bal.	0.96	0.02
Excess-Si Alloy B	0.64	0.01	0.81	< 0.01	< 0.01	< 0.01	Bal.	0.95	0.45

and equilibrium β phases, the three phases were made to precipitate by subjecting the specimen sheets to a solutionizing treatment at 823K for 1.8ks, water quenching and immediately after that, the following artificial aging treatments. The conditions of the artificial aging treatments were as follows: at 448K for 32.4ks (near the maximum hardness) for forming the β'' phase; at 523K for 3.6ks (an overaging stage) for the β' phase; and at 623K for 7.2ks (same) for the equilibrium β phase. The heating rate was set at 20K/minute, and the state of precipitation was measured using a differential scanning calorimeter (DSC).

Thin film specimens for transmission electron microscopy (TEM) were prepared by polishing the 1-mm-thick specimen sheets after the aging treatment to 50 μ m by machining and electrolytically polishing them in a 2-to-1 solution of methanol and nitric acid cooled to 253K.

The precipitates were characterized through structural and chemical analyses using a field emission type TEM (HF-2000 made by Hitachi Ltd.) having an acceleration voltage of 200keV and the function of energy dispersive X-ray spectroscopy (EDS). The EDS standard-less method by keveX-QUANTEX was employed for the quantitative chemical analysis of the precipitates, and nanometer-probe electron diffraction for the structural analysis.

3. Results and Discussion

Fig. 1 shows DSC curves of three specimens of Alloy B that underwent the following treatments, respectively: (a) the solutionizing treatment and quenching; (b) the solutionizing treatment, quenching

and aging treatment at 448K for 32.4ks; and (c) the solutionizing treatment, quenching and aging treatment at 523K for 3.6ks. Based on study reports that employed thermal analysis and TEM observation in combination^{2,10,11}, the authors assumed that the exothermic peaks of the DSC curves near 360, 540 and 580K corresponded to the precipitation of the G.P.I zone and β'' and β' phases, respectively, and the endothermic peaks near 490 and 550K to the dissolution of the G.P.I zone and β'' phase, respectively.

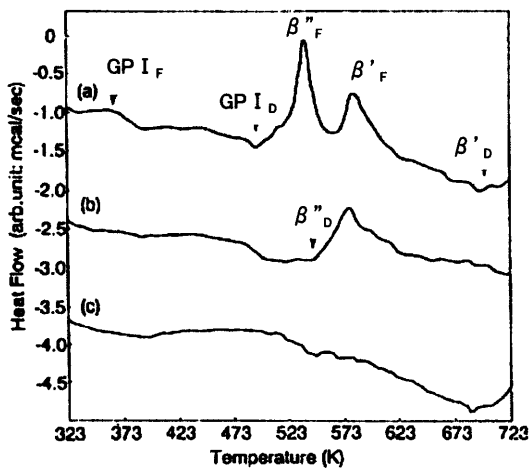
Whereas the DSC curve (a) of the solutionized and quenched specimen has an exothermic peak near 540K corresponding to the precipitation of the β'' phase and another near 580K corresponding to the precipitation of the β' phase, the curve (b) of the specimen aged at 448K after the solutionizing and quenching lacks any exothermic peak corresponding to the precipitation of the β'' phase, and instead, it has an endothermic peak near 550K corresponding to the dissolution of the β'' phase. In addition, the curve (c) of the specimen aged at 523K after the solutionizing and quenching lacks any exothermic peak near 580K corresponding to the precipitation of the β' phase. This was substantially the same with the specimens of Alloy A, though the temperatures of the peaks were somewhat different. Based on the DSC analysis results, the main precipitation phases of the specimens aged at 448 and 523K were judged to be the β'' and β' phases, respectively, either for Alloy A or B.

3.1 Structure of precipitate β'' phase in specimen aged at 448K

Needle-shaped precipitates of the β'' phase were observed in a large quantity in the specimens of Alloys A and B aged at 448K. Fig. 2 shows a high resolution electron micrograph (crystal lattice image), a nanometer-probe electron diffraction pattern and a selected area electron diffraction pattern of a β'' precipitate observed in the specimen of balanced Alloy A aged at 448K, all taken in the longitudinal direction of the needle shape. The incidence of the beam was in the $\langle 0\ 0\ 1 \rangle_{\alpha\text{-Al}}$ direction. Analysis of the nanometer-probe electron diffraction pattern in Fig. 2(b) revealed that the crystal lattice of the precipitate of β'' phase was monoclinic with lattice constants of $a = 0.714 \pm 0.017$ nm, $b = 0.658 \pm 0.013$ nm, $c = 0.405$ nm and $\gamma = 75 \pm 1^\circ$, and that the precipitate had a crystal orientation relationship with the matrix α -Al phase of $(1\ 0\ 0)_{\beta''} // (3\ -1\ 0)_{\alpha\text{-Al}}$, $(0\ 1\ 0)_{\beta''} // (2\ 3\ 0)_{\alpha\text{-Al}}$. Since there are four equivalent orientations for each of the three $\langle 1\ 0\ 0 \rangle_{\alpha\text{-Al}}$ orientations of the matrix α -Al phase, there are 12 possible orientation relationships in total. A similar electron diffraction pattern was obtained with the β'' phase of excess-Si Alloy B, and the crystal lattice and lattice constants were found to be the same as those of the β'' phase of Alloy A.

3.2 Structure of precipitate β' phase in specimen aged at 523K

Rod-shaped precipitates of the β' phase having two crystal lattice, hexagonal and orthorhombic, were observed in the specimens aged at 523K of both Alloys A and B. The β' phase having the hexagonal lattice roughly corresponds with that in the report by Matsuda et al.¹². Regarding the β' phase having the orthorhombic lattice, on the other hand, Fig. 3 shows a typical nanometer-probe electron diffraction pattern and a schematic representation. The lattice constants were calculated from the diffraction pattern as $a = 0.672 \pm 0.003$ nm, $b = 0.787 \pm 0.003$ nm and $c = 0.405$ nm, and the orientation relation-



G.P.I_F : formation of G.P.I zone
 G.P.I_D : dissolution of G.P.I zone
 β''_F : formation of β'' phase
 β'_F : formation of β' phase
 β''_D : dissolution of β'' phase
 β'_D : dissolution of β' phase

Fig. 1 DSC curves for the Alloy B as solutionized and quenched (a), aged at 448K for 32.4ks (b), and aged at 523K for 3.6ks (c)

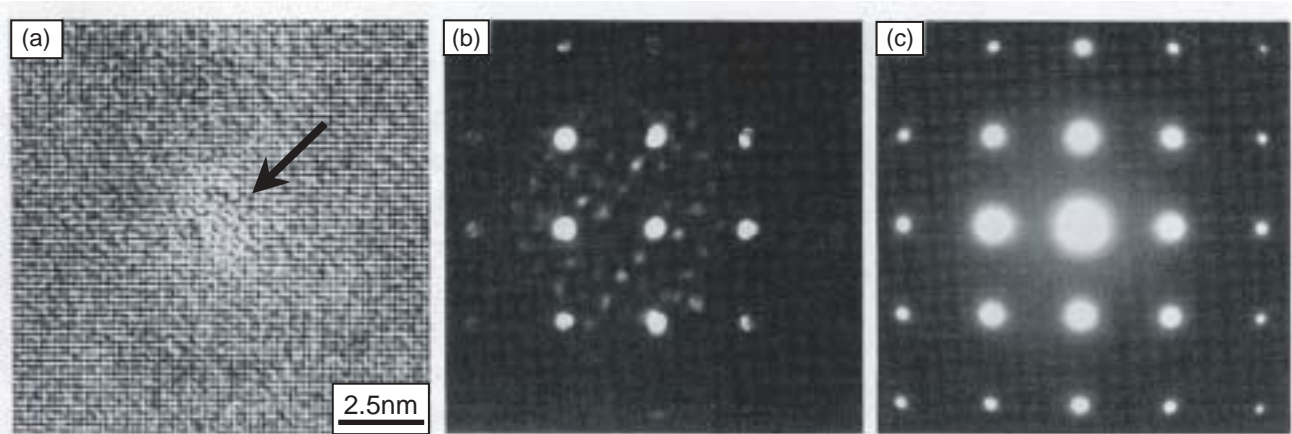


Fig. 2 High resolution electron micrograph (a), nano-diffraction pattern (b), and selected area diffraction pattern (c) of β'' phase in the Alloy A aged at 448K for 32.4ks

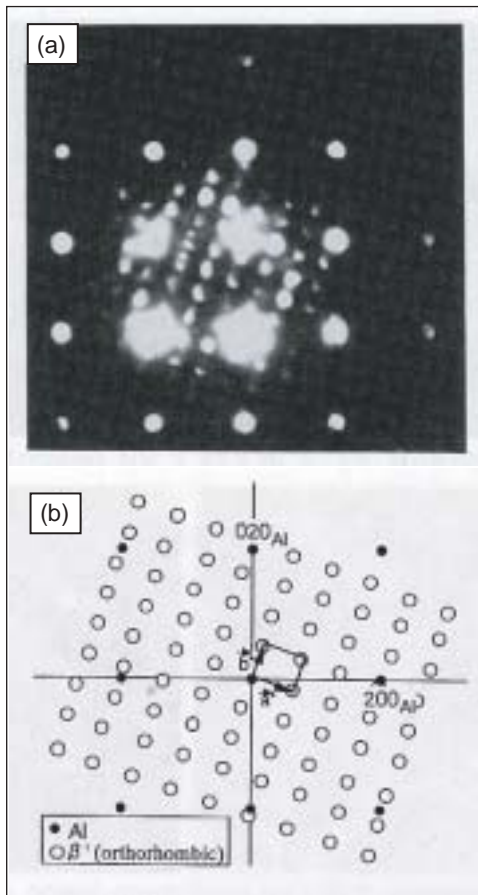


Fig. 3 Nano-diffraction pattern of an orthorhombic type β' phase (a) and the schematic representation (b) The electron beam direction was $\langle 0 0 1 \rangle_{\alpha-Al}$.

ship was found to be $(1 0 0)_{\beta'} // (3 -1 0)_{\alpha-Al}$. Table 2 summarizes the crystal lattice and the orientation relationships with the matrix α -Al phase of the β'' and β' phases.

3.3 Composition analysis of precipitation phases by nanometer-probe EDS

The β'' and β' phases in the specimens aged at 448 and 523K of both Alloys A and B were analyzed by the nanometer-probe EDS. Since a CaF_2 type equilibrium β phase had been found in the specimens aged at 623K, the chemical composition of this β phase was also analyzed for comparison purposes. The electron beam was aligned to the $\langle 0 0 1 \rangle_{\alpha-Al}$ direction (longitudinal direction) of the precipitates. Fig. 4 shows crystal lattice images and nanometer-probe EDS spectrums of the β'' phase in the specimen aged at 448K and the β' phase in that aged at 523K. As seen in the graphs, clear peaks were found in precipitates several nanometers in size, and the peaks were identified to be those of Mg and Si. Incidentally, the Al peaks in the profile diagrams are presumed to be those of the Al matrix. The Mg/Si composition ratios (in atomic ratios) of the precipitate phases were calculated as follows: in order to eliminate the influence of the Al matrix, a linear regression equation was established for each of the Mg-Al and Si-Al concentration relationships, and the respective values of the intercepts of these equations at Al concentration = 0 were defined as the concentration of Mg and Si.

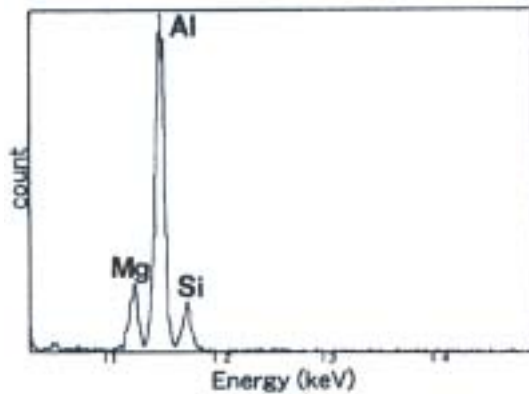
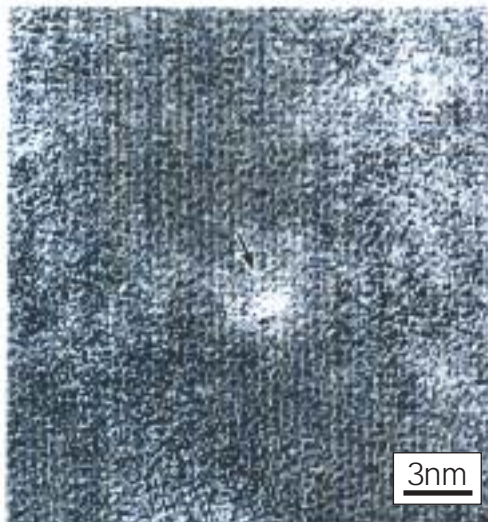
Table 3 shows the Mg/Si atomic ratios of the precipitate phases calculated in the above manner. Whereas the Mg/Si ratio of the β'' phase in the Alloy B specimen aged at 448K was approximately 1, that in the Alloy A specimen aged at the same temperature was nearly 2, showing a clear difference. What is more, whereas, among the specimens of excess-Si Alloy B, the Mg/Si ratio of the β' phase in the specimen aged at 523K was remarkably different from that of the β'' phase in the specimen aged at 448K, the composition ratios were substantially the same among the specimens of balanced Alloy A. Note that while the β' phase exists in both hexagonal and orthorhombic lattice, there was no difference in the Mg/Si atomic ratio between the two. The Mg/Si ratio of the equilibrium β phase found in the specimens aged at 623K of both Alloys A and B was approximately 2, the equilibrium composition ratio.

As stated earlier, the β'' phase has a monoclinic crystal lattice, and the β' phase has hexagonal and orthorhombic crystal lattice, and these phases are semi-coherent precipitation phases having specific orientation relationships with the matrix α -Al phase. The Mg/Si atomic ratios of these phases were found to deviate from the equilib-

Table 2 Crystal lattice of the precipitates, and orientation relationship between precipitates and α -Al

Precipitate	Crystal lattice	Orientation relationship
β''	Monoclinic $a = 0.714 \pm 0.017\text{nm}$, $b = 0.658 \pm 0.013\text{nm}$, $c = 0.405\text{nm}$, $\gamma = 75 \pm 1^\circ$	$(1\ 0\ 0)_{\beta''} // (3\ -1\ 0)_{\alpha\text{-Al}}$ $(0\ 1\ 0)_{\beta''} // (2\ 3\ 0)_{\alpha\text{-Al}}$
β'	Hexagonal $a = 0.705$, $c = 0.405\text{nm}$	$(-1\ 0\ 1\ 0)_{\beta'} // (2\ 0\ 0)_{\alpha\text{-Al}}$ $(-1\ 2\ -1\ 0)_{\beta'} // (0\ 2\ 0)_{\alpha\text{-Al}}$
		$(-1\ 1\ 0\ 0)_{\beta'} // (2\ 2\ 0)_{\alpha\text{-Al}}$ $(1\ 1\ -2\ 0)_{\beta'} // (2\ 2\ 0)_{\alpha\text{-Al}}$
		$(0\ 1\ -1\ 0)_{\beta'} // (3\ 1\ 0)_{\alpha\text{-Al}}$ $(2\ 1\ 1\ 0)_{\beta'} // (1\ 3\ 0)_{\alpha\text{-Al}}$
Orthorhombic $a = 0.672 \pm 0.003\text{nm}$, $b = 0.787 \pm 0.003\text{nm}$, $c = 0.405\text{nm}$	$(1\ 0\ 0)_{\beta'} // (3\ -1\ 0)_{\alpha\text{-Al}}$ $(0\ 1\ 0)_{\beta'} // (2\ 3\ 0)_{\alpha\text{-Al}}$	

(a) β'' phase in the Alloy A aged at 448K for 32.4ks



(b) β' phase in the Alloy A aged at 523K for 3.6ks

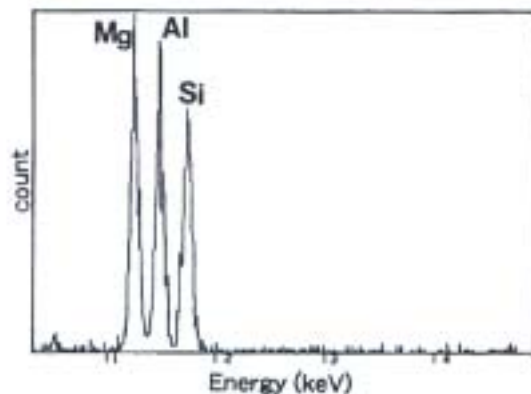


Fig. 4 High resolution electron micrographs and EDS spectrums of β'' and β' phase in the Alloy A. The electron beam direction was $\langle 0\ 0\ 1 \rangle_{\alpha\text{-Al}}$.

Table 3 Mg/Si atomic ratio of precipitates

Alloy	β'' phase (448K \times 32.4ks)	β' phase (523K \times 3.6ks)	β - Mg_2Si phase (623K \times 7.2ks)
Balanced Alloy A	1.74 ± 0.07	1.75 ± 0.03	2.10 ± 0.15
Excess-Si Alloy B	1.00 ± 0.04	1.21 ± 0.04	2.13 ± 0.05

rium composition ratio of 2 to the excessive-Si side in different extents depending on the alloy composition, the deviation being larger in excess-Si Alloy B. In spite of the difference in the Mg/Si ratio depending on the alloy composition, the crystal lattice of the β'' and β' phases are the same in Alloys A and B, and the lattice constants are substantially the same, too. This seems to indicate that the precipitation processes from a supersaturated solid solution through (a G.P.I zone,) an intermediate β'' phase and then an intermediate β' phase to an equilibrium β phase is not affected by alloy composition. An excessive addition of Si to a balanced alloy remarkably enhances the aging properties and form fine precipitate structures at paint baking temperatures. Presumably, this is largely due to the significant deviation of the Mg/Si ratio of the precipitate β'' phase from the equilibrium ratio of 2 to the excessive-Si side.

To promote the actual application of Al-Mg-Si alloys, Nippon Steel has designed bake-hardening type Al-Mg-Si alloys for automobile body applications in overall consideration of widely varied precipitation behavior of the material during aging that influences its bake-hardening. This paper gives a typical example of the basic knowledge on the precipitation behavior of the material.

4. Summary

The fine precipitates of Al-Mg-Si alloys were characterized in the present study by nanometer-probe electron diffraction employing a field emission type transmission electron microscope and by

nanometer-probe energy dispersive spectroscopy, and as a result, the following findings were obtained:

- (1) The β'' phase, which forms in both a balanced alloy and an excess-Si alloy as a result of an aging treatment at 448K, has a monoclinic crystal lattice, and on the other hand, the β' phase, which forms as a result of an aging treatment at 523K, has two crystal lattice, hexagonal and orthorhombic.
- (2) The Mg/Si composition ratios of the β'' and β' phases deviate from the equilibrium ratio of 2 to the excessive-Si side, the deviation being larger in an excess-Si alloy than in a balanced alloy.

References

- 1) Zhen, L., Kang, S.B.: Scripta Mater. 36, 1089 (1979)
- 2) Miao, W.F., Laughlin, D.E.: Scripta Mater. 40, 873 (1999)
- 3) Yamada, K., Sato, T., Kamio, A.: Light Metals. 30, 215 (2001)
- 4) Saga, M., Sasaki, Y., Kikuchi, M., Hibino, A., Matsuo, M.: Light Metals. 53 (11), 516 (2003)
- 5) Suzuki, H., Sugano, M., Shiraiishi, Y.: Light Metals. 28, 233 (1978)
- 6) Langerweger, J.: Proc. Aluminium Technology '86. Paper No.49, 1986, p.216
- 7) Thomas, G.: J. Inst. Metals. 90, 57 (1961-62)
- 8) Kelly, A., Nicholson, R.B.: Pro. Mater. Sci. 10, 151 (1963)
- 9) Lynch, J.P., Brown, L.M., Jacobs, M.H.: Acta Metall. 30, 1389 (1982)
- 10) Sugano, M., Suzuki, H., Shiraiishi, Y.: Light Metals. 28, 553 (1978)
- 11) Burger, G.B., Guputa, A.K., Jeffrey, P.W., Lloyd, D.J.: Mater. Charact. 3523 (1995)
- 12) Matsuda, K., Tada, S., Ikeno, S.: J. Electron Microsc. 42, 1 (1993)